ACS APPLIED MATERIALS & INTERFACES

Letter

www.acsami.org

Inorganic Photovoltaic Devices Fabricated Using Nanocrystal Spray Deposition

Edward E. Foos,*[,†] Woojun Yoon,[†,‡] Matthew P. Lumb,[†,§] Joseph G. Tischler,[†] and Troy K. Townsend[†,‡]

[†]Naval Research Laboratory, Washington, D.C. 20375, United States

[§]The George Washington University, 2121 I Street NW, Washington, D.C. 20037, United States

Supporting Information

ABSTRACT: Soluble inorganic nanocrystals offer a potential route to the fabrication of all-inorganic devices using solution deposition techniques. Spray processing offers several advantages over the more common spin- and dip-coating procedures, including reduced material loss during fabrication, higher sample throughput, and deposition over a larger area. The primary difference observed, however, is an overall increase in the film roughness. In an attempt to quantify the impact of this morphology change on the devices, we compare the overall performance of spray-deposited versus spin-coated CdTe-based Schottky junction solar cells and model their dark current−voltage characteristics. Spray deposition of the active layer results in a power conversion efficiency of 2.3 ± 0.3% with a fill factor of 45.7 ± 3.4%, V_{oc} of 0.39 ± 0.06 V, and J_{sc} of 13.3 ± 3.0 mA/cm^2 under one sun illumination.

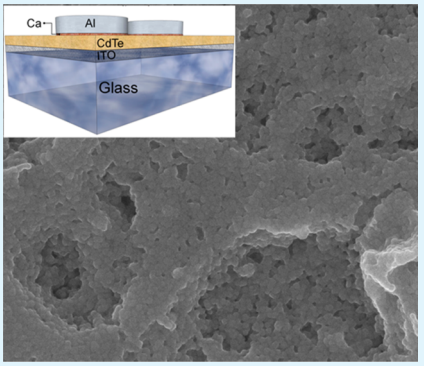

KEYWORDS: *photovoltaic, nanocrystal, processing, CdTe, spray, modeling*

INTRODUCTION

Inorganic nanocrystals are attractive elements for the fabrication of next-generation optoelectronic devices because of their inherent ability to harness the effects of quantum confinement, enabling the tuning of a broad range of electronic material properties through synthetic control over size. For this reason, semiconductor nanocrystals have been intensively studied for their application in photovoltaics,[1,2] light-emitting diodes,[3] and photodetectors.[4] In conjunction with these excellent electronic properties, the physical ability to manipulate these materials in solution provides an opportunity for the low-cost fabrication of a wide range of inorganic devices. As a specific example, the field of photovoltaics is expected to be influenced by the introduction of low-cost, moderate-efficiency alternatives to crystalline silicon, and colloidal quantum dot solar cells have been one focus of these efforts.[1] The fabrication of small-scale devices using thin films of these next-generation materials often relies on spin coating, a process that produces smooth uniform films but is inherently wasteful. This is especially problematic if used to deposit custom-synthesized or high-cost active layers over large areas and, in addition, is not immediately translatable to a high-throughput production process. For this reason, alternative material deposition technologies are needed.

Early reports on the use of nanocrystals in photovoltaic devices focused on blending spherically symmetric nanocrystals or elongated nanocrystals (i.e., nanorods) into a polymer matrix.[5−8] In this configuration, the nanorods functioned as the primary photon absorber, leading to the generation of excitons, while the polymeric host provided a means for electron−hole separation analogous to that of organic bulk heterojunction devices. The first report of an entirely inorganic device processed by spin coating was by Gur and co-workers,[9] who reported the use of densely packed nanorod films for the active layers, relying on the junction at the material interface between CdSe and CdTe for charge separation. Nanorods were chosen because the relaxed confinement in one dimension was expected to improve charge separation across the inorganic interface.[7,9] It was found that, in order to obtain devices with increasing power conversion efficiencies, however, the bulk of the organic ligands needed to be removed via a sintering process, which dramatically increased the short-circuit current densities. Subsequent work demonstrated that this process increased the grain size of the inorganic components.[10] While this procedure limits any possible benefits of quantum confinement because the sintered inorganic layers behave similarly to bulk, the potential to solution-process inorganic devices using this methodology is potentially very interesting. More recent approaches, largely focused on lead chalcogenides, have examined the exchange of nanocrystal surface ligands with bifunctional molecules to prepare devices by dip or spin coating.[11,12] Spray coating via an airbrush has also been shown to be a useful alternative to spin coating for the deposition of thin films of inorganic nanomaterials.[13−15] While the film uniformity and roughness are subject to more variability, the resulting devices show remarkable tolerance to these differ-

Received: June 21, 2013
Accepted: September 5, 2013
Published: September 5, 2013

 © 2013 American Chemical Society

Table 1. Summary of the Performance of Metal (Ca/Al)−CdTe Nanocrystal Schottky Junction Solar Cells (ITO/CdTe/Ca/Al) in the Dark and under AM1.5G-Filtered Spectral Illumination (100 mW/cm^2)[a]

device	average thickness (nm)	RMS roughness (nm)	J_0 (A/cm^2)	n (diode ideality factor)	R_sA (Ω·cm^2)	$R_{sh}A$ (Ω·cm^2)	J_{sc} (mA/cm^2)	V_{oc} (V)	FF (%)	efficiency (%)
spin	435	3.9	$(1.0 \pm 0.9) \times 10^{-7}$	2.8 ± 0.5	69 ± 15	$(5.1 \pm 3.9) \times 10^4$	13.2 ± 0.2	0.53 ± 0.02	43.1 ± 4.2	3.0 ± 0.3
spray	510	202	$(3.0 \pm 0.3) \times 10^{-5}$	4.2 ± 1.7	37 ± 10	$(5.4 \pm 3.3) \times 10^3$	13.3 ± 3.0	0.39 ± 0.06	45.7 ± 3.4	2.3 ± 0.3

[a]The values of J_0, n, R_s, and R_{sh} are defined in eq 1.

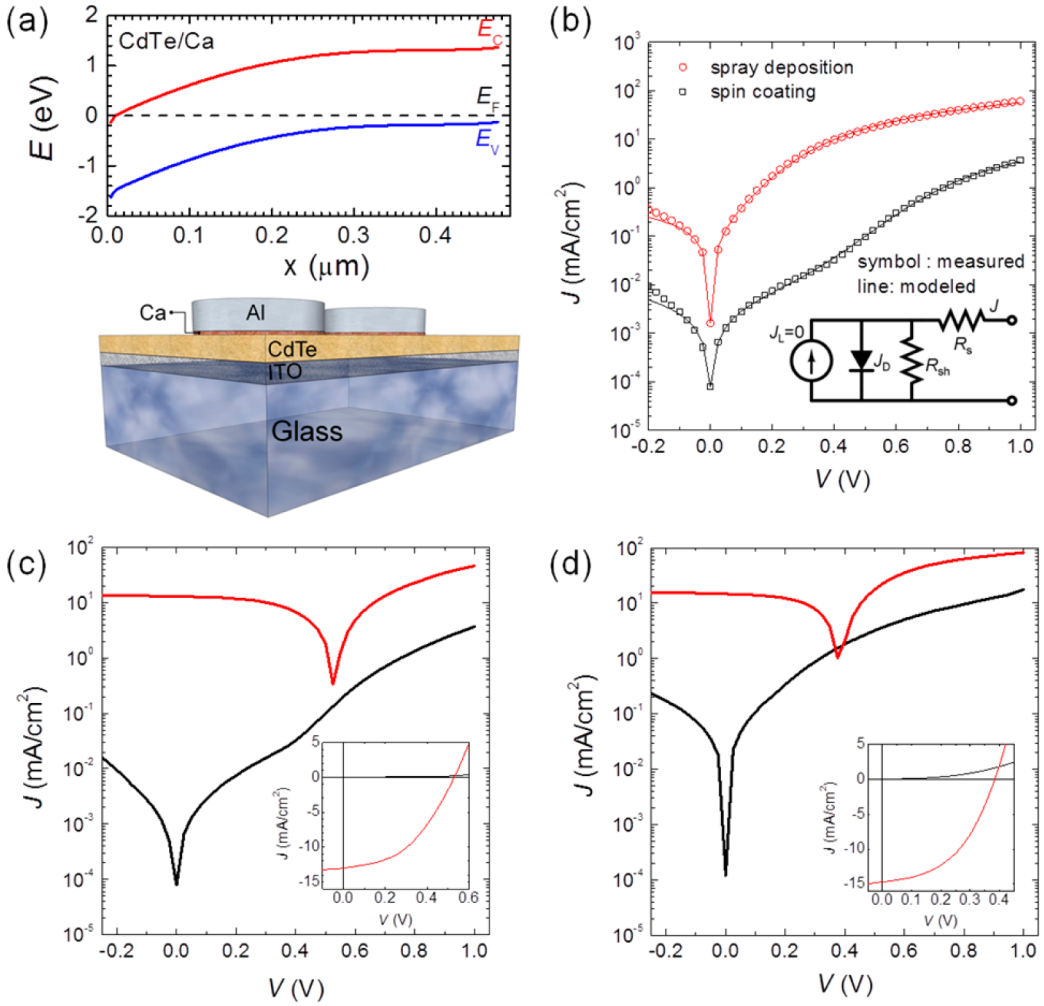

Figure 1. (a) Energy band model under zero bias and schematic of the metal−CdTe nanocrystal Schottky junction solar cells. The energy band diagram shows the presence of a Schottky barrier and band bending in the conduction band (red) and valence band (blue) near the interface between the calcium contact and the CdTe nanocrystal film. (b) Measured and modeled dark J−V curves of solar cells fabricated through spin and spray coating. The open symbol is the measured data, while the solid lines are modeled according to eq 1. The inset shows the equivalent circuit of a solar cell. J−V characteristics in the dark (black) and under AM1.5G-filtered spectral illumination (100 mW/cm^2) (red) of solar cells fabricated through (c) spin coating and (d) spray coating. The area of the cell is 0.1 cm^2.

ences. Herein we report Schottky-barrier solar cells composed of CdTe nanocrystals, where the active layer is fabricated by a spray-coating process, yielding devices with a power conversion efficiency of 2.3 ± 0.3% under one sun illumination.

EXPERIMENTAL SECTION

All reactions were conducted under inert conditions using standard Schlenk techniques unless otherwise noted. Oleic acid (90%), 1-octadecene (90%), and trioctylphosphine (TOP; 90%) were purchased from Aldrich. CdO (99.99%) and tellurium (99.8%) were purchased from Strem. All reagents were used as received without further purification.

Nanocrystal Synthesis. The CdTe nanocrystals were synthesized according to a published procedure[16] with additional details provided in the Supporting Information. Following isolation from the reaction, all solid was dissolved in 5 mL of pyridine and transferred to a round-bottomed flask fitted with a vacuum adaptor. The head space over the solution was evacuated and backfilled with argon five times, and the solution was lowered into a 85 °C oil bath and stirred overnight. This ligand-exchange step was performed to reduce the amount of oleate ligand present on the nanocrystal surface. Following exchange, the solution was then added to 40 mL of heptane, causing an immediate precipitation. The solid was isolated by centrifugation (2500 rpm; 5 min) and redissolved in 10 mL of 1:1 (v/v) pyridine/1-propanol.[16] The concentration of the CdTe stock solution was determined to be 40 mg/mL.

Device Fabrication. All device samples were fabricated in air on indium−tin oxide (ITO; sheet resistance of 8−12 Ω/sq)-coated glass substrates (25 × 25 × 0.7 mm) obtained from Delta Technologies. The substrates were rinsed with EtOH, dried under a stream of N_2, and cleaned via UV/ozone (12 min; 150 °C; 0.5 L/min flow rate) immediately prior to film deposition. The spin-coating procedure was conducted as reported in the literature using the 40 mg/mL stock solution.[16,17] For spray-coated samples, the concentrated stock solution was diluted to approximately 1 mg/mL in $CHCl_3$. Substrates were mounted vertically and warmed to 80 °C. The spray solution was loaded into the airbrush and applied uniformly to the substrate using a pressure of 20 psi N_2.[13] After 5 mL had been deposited, the substrate was removed from the sample mount and dried on a 150 °C hot plate for 2 min. It was then immersed quickly in a saturated solution of $CdCl_2$ in MeOH warmed to 60 °C and rinsed three times in iPrOH. The substrate was blown dry with N_2 and placed on a 400 °C hot plate in air for 1 min. After cooling to room temperature, the sample was remounted and the procedure repeated until all CdTe spray solution had been used. Following material deposition through either spin or spray coating, the devices were completed by a sequential thermal evaporation of calcium (20 nm) and aluminum (80 nm) using a shadow mask. The active area of the cells was 0.1 cm^2. Note that the sintered CdTe layer was not rinsed with deionized water prior to metal evaporation.

Device Characterization. The dark and light current density−voltage (J−V) characteristics were measured with a semiconductor parameter analyzer (Agilent 4145B) in air without any device encapsulation. The solar cell efficiency was measured under the spectral output from a 150 W solar simulator (Newport) using an air mass 1.5 global (AM1.5G) filter. The irradiance (100 mW/cm^2) of the solar simulator was adjusted using a standard silicon photodetector (Newport, 818-SL-L) that had been cross-calibrated by a reference silicon cell traceable to the National Renewable Energy Laboratory. For each substrate, six individual devices were measured and averaged to obtain the results in Table 1.

RESULTS AND DISCUSSION

The metal−CdTe Schottky junction solar cells shown in Figure 1a were prepared for comparison of their performance following either spray or spin fabrication. This architecture was chosen to simplify the optimization and comparison of the CdTe layers prepared under different fabrication conditions. Previously, we found spray coating to produce films comparable to those from spin coating when the spray solution was dilute (≤0.5 mg/mL) and composed of low-solubility aggregates.[13] Under these prior conditions, film thicknesses were minimized (<200 nm) to compensate for the overall low carrier mobility of the ligand-encapsulated nanorods. The current structures differ from these early attempts in the following ways: (1) Spherical nanocrystals were used in place of nanorods. (2) The solution concentrations were higher (≥1 mg/mL). (3) The CdTe absorber layer thicknesses were greater than 200 nm. (4) A single material Schottky junction structure was used instead of a heterojunction. As a consequence of no. 1, the material was of much higher solubility in the organic solvent used for the depositions, permitting improved control over the layer thickness. Following film deposition, a $CdCl_2$-based sintering treatment was utilized to increase the grain size and improve the overall performance.[9,10,16] This results in a solution-processed device composed entirely of inorganic material where the contributions from quantum confinement effects are minimal.

The spin-coated devices were fabricated based on a recently reported "layer-by-layer" approach[16] designed to minimize cracking and pinhole formation during the fabrication process. Briefly, the CdTe nanocrystal stock solutions were spun onto cleaned ITO substrates. Following a single spinning cycle, the substrate was dried and then dipped into a saturated solution of $CdCl_2$ in MeOH. After rinsing and drying with N_2, the substrate was placed on a 400 °C hot plate in air for 10 s. An additional nanocrystal layer was spun on top, and this process repeated until the desired layer thickness had been achieved. For films of ∼500 nm thickness, this was found to be 10 cycles. The spray-coated devices were prepared similarly but with several modifications. First, the stock solutions used for spin coating were diluted with $CHCl_3$ to an approximate concentration of 1 mg/mL. Because of rapid evaporation of the solvent when sprayed on a heated substrate, as well as the increased efficiency of material transfer, the spray solutions require lower overall concentrations to obtain acceptable roughness values.[13] The ITO substrates were mounted vertically and warmed to 80 °C, followed by airbrush application of the nanocrystal solution. Four times during the spraying process the samples were removed, dried, and treated with $CdCl_2$ as described above. These thicker films were sintered in air for 1 min at 400 °C. The substrates were then remounted, and the procedure was repeated until all of the nanocrystal solution had been deposited.

Figure 2 shows scanning electron microscopy (SEM) images of the surface of films prepared by spin and spray coating for

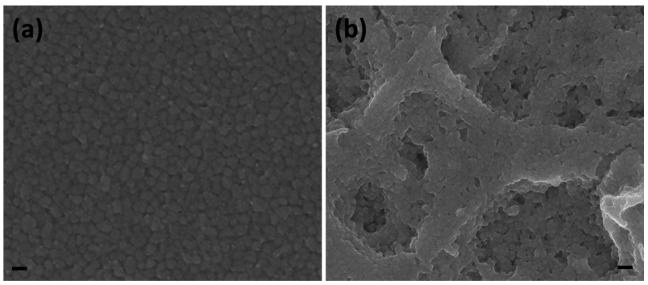

Figure 2. SEM images of the top surface of the deposited films following deposition and sintering, showing (a) CdTe spin coated and (b) CdTe spray coated. The scale bar in both images represents 200 nm.

comparison of the deposition techniques. The surface morphology clearly indicates that the spray-coating process produces a rougher surface than that produced by spin coating of the same material. In addition, the CdTe films are composed of grains approximately 100 nm in size. The absorbance spectra shown in Figure 3 of the CdTe nanocrystals used in the process indicate an average diameter of ∼4 nm through the use of a published empirical function.[18] Consistent with growth of the grain size and the loss of quantum confinement, the absorbance spectra of the sintered CdTe films show an absorbance onset at approximately 825 nm, very close to the bulk value of 827 nm. This growth in grain size is attributed to the sintering process used on the films and is consistent with previous results.[10] Film thickness and roughness data obtained for the samples using optical profilometry are listed in Table 1.

The Schottky junctions were fabricated through evaporation of a low-work-function Ca/Al metal contact on top of the sintered CdTe nanocrystal layer, as illustrated in Figure 1a. The dark J−V characteristics for the solar cells are shown in Figure 1b for both the spin- and spray-coated samples. In order to extract the saturation current, series resistance, and shunt resistance, the dark current density of the device is assumed to fit a one diode model as follows:

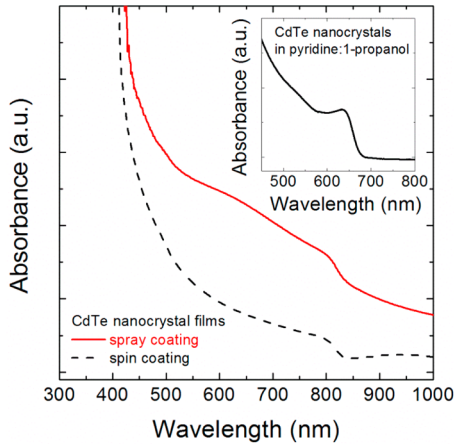

Figure 3. Absorbance data of sintered CdTe nanocrystals fabricated through layer-by-layer assembly using spin (dashed) and spray (solid) coating (glass/ITO/CdTe). The inset shows the absorbance of the stock CdTe nanocrystals in 1:1 (v/v) pyridine/1-propanol. The absorbance is without substrate correction.

$$J = J_0\left[\exp\left(\frac{q(V - JAR_s)}{nkT}\right) - 1\right] + \frac{V - JAR_s}{AR_{sh}} \quad (1)$$

where J_0 is the saturation current density (A/cm^2), R_s is the series resistance (Ω), R_{sh} is the shunt resistance (Ω), A is the device area (cm^2), and n is the ideality factor. As seen in Figure 1b, the solid lines are curves fitted according to eq 1, which are in good agreement with the measured data. Table 1 summarizes the experimental performance data. In an assessment of these dark parameters, the most noticeable feature is that the spray-coated devices showed a 2 orders of magnitude higher saturation current density. Because the same CdTe stock solution and Ca/Al metal contacts are used for the two devices, the observed differences are most likely a result of the deposition process. This is not surprising because the increased roughness of the films produces a larger surface area that could result in more nonradiative recombination centers due to surface states such as semiconductor dangling bonds, surface oxides, or residual organic ligands not removed by the sintering process. Although both procedures produce similar thickness films, the number of deposition cycles is only 3 in the spray process, meaning that the film experiences less exposure to a saturated $CdCl_2$ solution relative to the 10-cycle spin-coating process. While the series resistances were similar in both the spray- and spin-coated devices, the shunt resistance was 1 order of magnitude lower in the spray-coated device than in the spin-coated device. This could be the result of a lower-density CdTe film with additional void spaces within the layer that increase leakage current pathways in the sprayed film. This explanation is also supported by the higher absorbance measured in the spray-coated CdTe film despite the similar thickness, suggesting that there is additional scattering caused by these defects. In addition, the high surface roughness of the sprayed samples could also contribute to an increased leakage current across the metal−CdTe Schottky junction as a result of a less conformal coating by the metal as it is deposited. Under AM1.5G illumination at 100 mW/cm^2, the sprayed CdTe solar cells exhibited a power conversion efficiency of 2.3 ± 0.3% with a fill factor (FF) of 45.7 ± 3.4%, V_{oc} of 0.39 ± 0.06 V, and J_{sc} of 13.3 ± 3.0 mA/cm^2, as shown in Figure 1d and Table 1. The lower V_{oc} values in the spray-coated devices are due to increased J_0 compared to the spin-coated device presented in Figure 1c. Spin-coated Schottky devices with efficiencies as high as 5% have previously been reported for CdTe/Al junctions,[10] although nanorods were used in the fabrication process unlike the nanocrystals used here. The results demonstrate that for these films J_{sc} is relatively insensitive to the deposition technique, but the sprayed films exhibit increased dark currents that lead to a reduction in V_{oc}. In light of these results, optimizing the spray deposition process to reduce film defects could ultimately lead to a minimal reduction in the performance between the two techniques.

Finally, it is worth commenting on the material usage associated with these techniques. In terms of the deposition efficiency, calculated as the mass of CdTe present in solution compared to the mass deposited on a substrate, a value between 15 and 20% is typical for spray depositions conducted as described in the Experimental Section. In order to obtain as uniform a coating as possible, the spray is directed over the edges of the substrate during deposition, accounting for some of the observed loss. Constraining the deposition to the center of the substrate increases this yield to approximately 30%. A similar analysis cannot be performed for the spin-coated samples because the sintering procedure leads to a change in mass due to ligand loss and the addition of $CdCl_2$ to the system. Without this treatment, the film is subject to dissolution in the solvent upon subsequent spin cycles. A second method of quantifying the deposition efficiency, therefore, is to consider the total mass of CdTe required to coat a particular area with a film of defined thickness. For the 25 × 25 mm substrates used here and coated with approximately 500 nm of material, we calculate that spin coating requires 40 mg of CdTe, while spray coating requires 10 mg. These estimated values indicate that, by this metric, the spray-coating process is 4 times more efficient than spin coating. Given the roughness and performance differences noted above, the spray process clearly can be advantageous for certain materials and architectures and enables a wider variety of substrates to be utilized.

CONCLUSIONS

In summary, we have prepared single-layer Schottky-barrier solar cells using spray deposition of inorganic nanocrystals and obtained a J_{sc} of 13.3 ± 3.0 mA/cm^2, V_{oc} of 0.39 ± 0.06 V, and FF of 45.7 ± 3.4% and an overall power conversion efficiency of 2.3 ± 0.3%. The spray deposition results in a rougher film morphology that manifests itself as a 2 orders of magnitude higher saturation current density compared to spin coating. Further optimization of the spray process to reduce this surface roughness and limit the V_{oc} suppression should be possible and lead to comparable performances between the two deposition techniques. Importantly, the spray-coating process enables larger areas to be covered more efficiently, reducing waste of the active layer components, while enabling deposition on asymmetric substrates. These advantages should be of substantial interest as inorganic nanocrystal-based solar cells become increasingly competitive as third-generation devices.

ASSOCIATED CONTENT

Supporting Information

Details of nanocrystal synthesis, X-ray diffraction spectra of device films, and external quantum efficiency data. This material is available free of charge via the Internet at http://pubs.acs.org.

AUTHOR INFORMATION

Corresponding Author

*E-mail: edward.foos@nrl.navy.mil.

Notes

The authors declare no competing financial interest.

‡National Research Council Postdoctoral Research Associate at the U.S. Naval Research Laboratory.

ACKNOWLEDGMENTS

The Office of Naval Research is gratefully acknowledged for financial support. This work was conducted while W. Yoon and T. Townsend held National Research Council Postdoctoral Fellowships at the Naval Research Laboratory.

REFERENCES

(1) Debnath, R.; Bakr, O.; Sargent, E. H. *Energy Environ. Sci.* **2011**, *4*, 4870−4881.
(2) Tang, J.; Sargent, E. H. *Adv. Mater.* **2011**, *23*, 12−29.
(3) Demir, H. V.; Nizamoglu, S.; Erdem, T.; Mutlugun, E.; Gaponik, N.; Eychmüller, A. *Nano Today* **2011**, *6*, 632−647.
(4) Konstantatos, G.; Sargent, E. H. *Nat. Nanotechnol.* **2010**, *5*, 391−400.
(5) Huynh, W. U.; Peng, X.; Alivisatos, A. P. *Adv. Mater.* **1999**, *11*, 923−927.
(6) Greenham, N. C.; Peng, X.; Alivisatos, A. P. *Phys. Rev. B* **1996**, *54*, 17628−17637.
(7) Huynh, W. U.; Dittmer, J. J.; Alivisatos, A. P. *Science* **2002**, *295*, 2425−2427.
(8) Huynh, W.; Dittmer, J.; Teclemariam, N.; Milliron, D.; Alivisatos, A.; Barnham, K. *Phys. Rev. B* **2003**, *67*, 115326.
(9) Gur, I.; Fromer, N. A.; Geier, M. L.; Alivisatos, A. P. *Science* **2005**, *310*, 462−465.
(10) Olson, J. D.; Rodriguez, Y. W.; Yang, L. D.; Alers, G. B.; Carter, S. A. *Appl. Phys. Lett.* **2010**, *96*, 242103.
(11) Koleilat, G. I.; Levina, L.; Shukla, H.; Myrskog, S. H.; Hinds, S.; Pattantyus-Abraham, A. G.; Sargent, E. H. *ACS Nano* **2008**, *2*, 833−840.
(12) Luther, J. M.; Law, M.; Beard, M. C.; Song, Q.; Reese, M. O.; Ellingson, R. J.; Nozik, A. J. *Nano Lett.* **2008**, *8*, 3488−3492.
(13) Javier, A.; Foos, E. E. *IEEE Trans. Nano.* **2009**, *8*, 569−573.
(14) Schulz, D. L.; Pehnt, M.; Rose, D. H.; Urgiles, E.; Cahill, A. F.; Niles, D. W.; Jones, K. M.; Ellingson, R. J.; Curtis, C. J.; Ginley, D. S. *Chem. Mater.* **1997**, *9*, 889−900.
(15) Nanu, M.; Schoonman, J.; Goossens, A. *Nano Lett.* **2005**, *5*, 1716−1719.
(16) Jasieniak, J.; MacDonald, B. I.; Watkins, S. E.; Mulvaney, P. *Nano Lett.* **2011**, *11*, 2856−2864.
(17) Yoon, W.; Foos, E. E.; Lumb, M. P.; Tischler, J. G. Solution processing of CdTe nanocrystals for thin-film solar cells. *38th IEEE Photovoltaic Specialists Conference (PVSC)*, June 3−8, 2012, Austin, TX; IEEE: New York, 2012; pp 002621−002624.
(18) Yu, W. W.; Qu, L.; Guo, W.; Peng, X. *Chem. Mater.* **2003**, *15*, 2854−2860.